ISSN: 2639-7536

Research Article

Petroleum and Chemical Industry International

New Risk Assessment Method of Gas Influx Based on Fifteen Example Wells

Xiaohui Wang[1,2], Zhichuan Guan[1], Yang Tian[1], Roman Shor[2]*

[1]*China University of Petroleum, Qingdao, Shandong 266580, China*

[2]*University of Calgary, Calgary, AB T2N 1N4, Canada*

***Corresponding author**
Roman Shor, University of Calgary, Calgary, AB T2N 1N4, Canada, E-mail: lunaryyt@163.com

Submitted: 13 Nov 2018; **Accepted**: 25 Nov 2018; **Published**: 05 Jan 2019

Abstract

With the increase of global deepwater drilling, the scale of the deepwater drilling contract market continues to expand, and the depth of the drilling operations constantly refreshes the record. At the same time, the drilling environment and related geological conditions becomes more and more complex, which leads to the increase of the risk in the operation of deepwater drilling. After the happening of "Deepwater Horizon Accident" in the Gulf of Mexico, the prevention and control of blowout has become an urgent problem to be solved in the development of offshore oil and gas. Dealing with the problem of overflow and blowout in deepwater drilling, the most effective technical measures are based on early detection and identification of gas influx. The research on the degree of gas invasion is the basis of the formulation and implementation of well control measures. In this paper, a simulation model of gas-liquid two-phase flow after the happening of gas influx is established to calculate the cross section gas content, mud tank overflow, and bottom-hole pressure. Through the calculation, the real-time quantitative relationship between the characterization of the gas content and the bottom-hole pressure and the increment of the mud pool was established, and then the real-time quantitative degree of gas invasion is analyzed.

Keywords: Deepwater drilling, gas invasion, real-time detection, numerical simulation, well control.

Introduction

With the continual discoveries of significant oil and gas field in deep water areas, global deepwater oil and gas exploration constantly heats up, and the investment in deepwater oil and gas exploration and development continues to increase. According to Yang (2014), the investment of global deepwater oil and gas exploration and development totaled $112 billion from 2008 to 2012, and the investment is expected to reach $223 billion from 2012 to 2017, which is doubled over the last five years [1]. And the investment of deep water well drilling and completion is expected to be $78 billion.

China is a maritime country, and as an important deep-water oil and gas development zone, South China Sea plays a decisive role in the energy replacement. In recent years, China has actively developed its own deepwater oil and gas development plan and took a series of deepwater oil and gas equipment and key technologies as national major research projects, which has made some achievements [2,3]. In 2010, the sixth generation China offshore drilling platform "offshore oil 981" of China National Offshore Oil Corporation (CNOOC) has been successfully undocked in Shanghai Waigaoqiao Shipbuilding Co. Ltd. In this year, CNOOC offshore capacity is more than 5000*104 t, completing the construction of "maritime Daqing [4].

As the depth of the seawater and drilling operations increases, the drilling environment and related geological conditions becomes more and more complex, this leads to the increase of the risk in the operation of deepwater drilling [5]. In 2010, the Gulf of Dalian oil pipeline explosion caused more than 1 thousand and 500 tons of oil leakage into the Gulf of Dalian, China, and this accident was a great threat to the sea water quality, ecosystem, and marine organisms, which finally affected the local fishery, tourism, and nearby residents. In the same year, the event of "Deepwater Horizon Accident" in the Gulf of Mexico caused a sensation all over the world [6,7]. The disastrous consequences to the ecological environment in this accident caused a serious threat to the Gulf of Mexico's energy strategy and the economic status, which brought painful blow to Mexico Bay area and influenced the life of the residents in the Mexico Bay area. What is more, BP Company and BP shareholders suffered heavy losses [8].

In case of dealing with the problem of overflow and blowout in deepwater drilling, the most effective technical measures are based on early detection and identification of gas influx [9]. There are many research institutions now testing and developing the technology of Detection Method on Marine Riser (DMOMR) to detect gas invasion as soon as possible [10,11]. Considering the serious consequences of gas invasion, even one minute to monitor the occurrence of gas invasion in advance, for the latter part of the well control work is of great significance.

CNOOC Research Institute, Beijing, and China University of Petroleum, Beijing, have been conducting 3 research projects to develop a gas kick detecting equipment on the riser and testing

its signal response. Letton Hall Group had developed a method to testing the density of the drilling fluid using the ultrasonic signals just above the wellhead, at the basis of subsea riser in 2015, aiming to detect the kick earlier than the conventional gas invasion monitoring method at the platform. Through the past ten years, detecting the gas influx in the marine section can be realized [3].

After the early detection and identification of gas influx, the reasonable well control plan will be put forward according to the risk degree. The research on the degree of gas invasion is done on the basis of the formulation and implementation of well control measures and at present, there is a lack of research and discussion on this problem. In this paper, an extended two-fluid model (TFM) is developed to describe the gas-liquid two-phase flow when gas influx occurs to calculate the cross section void fraction, mud tank overflow, and BHP. Avelar, C. S. presented a mathematical modeling of a proposed gas kick simulator and made a comparison between simulated and measured results for a test well located in Brazil [12,13]. Using the mathematical model, a sensitivity analysis regarding the effect of water depth in well control parameters has been done. Wang, Z. Y. built a simulation model for deepwater gas kicks with consideration of the hydrate phase transition [14]. This model includes the multiphase flow governing equations and the hydrate phase transition calculation equations. Through the calculation, the real-time quantitative relationship between the characterization of the void fraction and the BHP and the increment of the mud pool was established, and then the real-time quantitative degree of gas invasion is analyzed.

Methodology

The fluid flow in the annular when gas influx occurs is generally simplified to a two-phase flow as the low level of cuttings, and it was modeled based on the two-fluid model [15,16]. The major extension from previous gas influx models includes the addition of a modified temperature field of fluid in the annular and several assistant equations [17].

Governing Equations

The equation set describes the mass/momentum conservation of intrusive gas and drilling fluid, and the equations of heat transfer and equilibrium.

Immiscible intrusive gas/drilling fluid flow equations

The hypothesis based on the properties of drilling fluid and the surrounding factors are as follows: 1) one-dimensional unsteady flow in the wellbore; 2) compressible gas, incompressible liquid; 3) no mass transfer between liquid and gas; 4) a rigid drill string; 5) concentric drill string and borehole; 6) neglect of annular pressure [18,19]. The mass conservation equations for immiscible gas and liquid phases can be written as Equation (1) and Equation (2):

$$\frac{\partial(\rho_g E_g)}{\partial t}+\nabla\cdot(\rho_g E_g \boldsymbol{v_g})=S_g \qquad (1)$$

$$\frac{\partial[\rho_l(1-E_g)]}{\partial t}+\nabla\cdot\left[\rho_l(1-E_g)\boldsymbol{v_l}\right]=0 \qquad (2)$$

Where p_g is the gas density (kg/m^3); E_g is the gas-bearing ratio (dimensionless); $\boldsymbol{v}_g$ is the gas velocity (m/s); S_g is the gas source term (kg/(s•m^3)); p_l is the liquid or drill fluid density (kg/m^3); $\boldsymbol{v}_l$ is the liquid or drill fluid velocity (m/s). Then the total mass conservation equation of the fluid in the wellbore can be obtained:

$$\frac{\partial\left[\rho_g E_g+\rho_l(1-E_g)\right]}{\partial t}+\nabla\cdot\left[\rho_g E_g \boldsymbol{v_g}+\rho_l(1-E_g)\boldsymbol{v_l}\right]=S_g \qquad (3)$$

Momentum conservation law governs the flow rate of each phase:

$$\frac{\partial\left(\rho_g E_g \boldsymbol{v_g}\right)}{\partial t}+\nabla\cdot(\rho_g E_g \boldsymbol{v_g}^2)=div\left(E_g I_g\right)+\rho_g \boldsymbol{b}+\boldsymbol{m_g} \qquad (4)$$

$$\frac{\partial\left[\rho_l(1-E_g)\boldsymbol{v_l}\right]}{\partial t}+\nabla\cdot\left[\rho_l(1-E_g)\boldsymbol{v_l}^2\right]=div\left[(1-E_g)I_l\right]+\rho_l \boldsymbol{b}+\boldsymbol{m_l} \qquad (5)$$

where I_g is the stress tensor of gas phase (Pa); $\boldsymbol{b}$ is the unit mass force (m/s^2); $\boldsymbol{m}_l$ is the acting force to gas (kg/(m^2•s^2)); is the stress tensor of liquid phase (Pa); is the acting force to liquid (kg/(m^2•s^2)). The total momentum conservation equation of the fluid in the wellbore can be obtained when Equation (4) and Equation (5) are added together.

$$\begin{aligned}&\frac{\partial\left[\rho_g E_g \boldsymbol{v_g}+\rho_l(1-E_g)\boldsymbol{v_l}\right]}{\partial t}+\nabla\cdot\left[\rho_g E_g \boldsymbol{v_g}^2+\rho_l(1-E_g)\boldsymbol{v_l}^2\right]\\&=div\left[E_g I_g+(1-E_g)I_l\right]+(\rho_g+\rho_l)\boldsymbol{b}\end{aligned} \qquad (6)$$

Intrusive Gas/Drilling Fluid Energy Equations

In order to describe the temperature field of this deep water drilling system, it should be divided into 3 parts (see Figure 1) as follows: (1) the interior of drill string; (2) the annular between formation and drill string; (3) the annular between seawater and drill string.

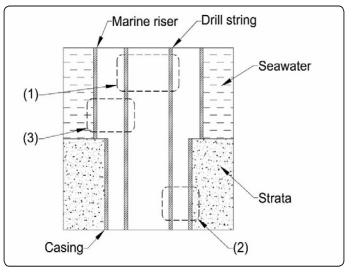

Figure 1: Regional drill pipes and divided heat transfer models

The energy flowing into an element carried by the drill fluid is as follows:

$$Q_p(z)=c_l\rho_l(z,t)VT_p(z,t) \qquad (7)$$

Where Q_p is the energy flowing into an element (W); c_l is the specific heat capacity of liquid or drill fluid (J/(kg•K)); V is the volume of the element and can be calculated as a cylinder volume (m^3). The energy flowing out the element carried by the drill fluid is as follows:

$$Q_p(z+dz)=c\rho(z,t)VT_p(z,t)+\frac{\partial[c\rho(z,t)VT_p(z,t)]}{\partial z}dz \qquad (8)$$

Therefore, the net energy flowing into an element carried by the drill fluid is

$$Q_p(z)-Q_p(z+dz)=-\frac{\partial[c\rho(z,t)VT_p(z,t)]}{\partial z}dz \qquad (9)$$

The energy from the annular space to the outer wall of the drill string equals the energy from the outer wall of the drill string to its internal wall, and the energy from the internal wall of the drill string to the interior of drill string, which is shown as follows:

$$Q_{qp}=h_{po}\pi d_{po}dz[\Delta T_a(z,t)-\Delta T_{po}(z,t)] \qquad (10)$$

$$Q_{ap} = \frac{2\pi\lambda_p dz[\Delta T_{po}(z,t) - \Delta T_{pi}(z,t)]}{\ln(d_{po}/d_{pi})} \quad (11)$$

$$Q_{ap} = h_{pi}\pi d_{pi} dz[\Delta T_{pi}(z,t) - \Delta T_p(z,t)] \quad (12)$$

where d_{pi} is the inside diameter of drill string (m); ΔT_{po} is the temperature difference in the outer wall of drill string (K); ΔT_{pi} is the temperature difference in the internal wall of drill string (K); ΔT_p is the temperature difference in the drill string (K); h_{pi} is the convection heat transfer coefficient of drill string and inside drill fluid (W/(m²•K)); d_{po} is the outside diameter of drill string (m); h_{po} is the convection heat transfer coefficient of drill string and annular drill fluid (W/(m²•K)); λ_p is the thermal conductivity of drill string (W/(m•K)); ΔT_{pa} is the temperature difference in annular (K). The ΔT_{po} and ΔT_{pi} can be eliminated according to Eqs. (10) and (11), and the net energy flowing into an element in the part of radial convection heat transfer can be therefore written as follows:

$$Q_{ap} = \frac{\pi[\Delta T_a(z,t) - \Delta T_p(z,t)]}{\frac{1}{h_{pi}d_{pi}} + \frac{1}{h_{po}d_{po}} + \frac{\ln(d_{po}/d_{pi})}{2\lambda_p}} \quad (13)$$

We did the numerical simulation based on the above data, and the law of gas-liquid two-phase flow was then obtained.

Results and Discussion

Validation of the Model

Evaluation for validation of each fluid model from the literature was already given in the respective study in the references. In order to validate the integrated model in this paper, the simulation results of this study for the overflow were compared with the actual data of a well in the South China Sea as a validation process. The related drilling parameters of the well are shown in Table 2 [20].

Table 2: Drilling parameters

Water depth/m	1298	Wellbore depth/m	3630
Drill pressure/t	4~ 6	Rotate speed/rpm	50
Torque/kN·m	13~15	Delivery rate/(L/s)	2701
Pump pressure/MPa	5.2	Mean drill speed/ (m/h)	10.8
Diameter of drill collar /mm	120.7	Diameter of non-magnetic drill collar/mm	120.7
Diameter of heavy weight drilling pipe /mm	88.9	Diameter of drilling pipe/ mm	127.0
Riser inner diameter/mm	482.6	Riser diameter/mm	533.4

Therefore, the energy conservation equation of part (1) in the deepwater drilling temperature system can be written as follows:

$$Q_p(z) - Q_p(z+dz) + Q_{ap} - \Phi_{f1} = \frac{\partial Q_p(z,t)}{\partial t} \quad (14)$$

Closure Relations

In order to make the equation set close, assistant equations such as equations of state, wall friction force, interfacial drag force, gas inflow rate, convective heat transfer coefficient equations, equations for viscosity and density of gas-liquid two-phase flow, and equations for temperature of seawater and strata are all included.

Boundary Condition

In the time when the drill bit just reaches the high-pressure gas reservoir area, the gas intends to inflow to the annular. Usually, the gas-bearing ratio and gas velocity are considered as 0 at that time, and the inlet gas and liquid flow rates and outlet pressure are known. Therefore, the corresponding liquid or drill fluid velocity equals the ratio of fluid flow rate and the annular area, and the transient pressure equals the relevant fluid column pressure. The pressure in wellhead can be considered as one bar.

Simulation Case

The consequence of gas influx detection is affected by numerous factors, such water depth, wellbore depth, permeability of the formation, and formation equivalent density. The data of an actual well M-1 located in South China Sea is presented in Table 1.

Table 1: Partial parameters of the formation and drilling operation

Water depth (m)	1500	Inner diameter of marine riser (mm)	475.74	Drill bit diameter (mm)	215.9	Formation permeability (mD)	100
Wellbore depth (m)	2500	Outer diameter of marine riser (mm)	508	Penetration rate (m/h)	8	Formation equivalent density (kg/m³)	1330
Drill fluid flow (m³/s)	0.03	Inner diameter of intermediate casing (mm)	222.38	Outer diameter of drill pipe (mm)	127	Sea surface temperature (°C)	15.0
Drill fluid density (kg/m³)	1100	Outer diameter of intermediate casing (mm)	244.5	Length of open hole portion (m)	350	Formation geothermal gradient (°C/100m)	3.2

The actual data presented that gas influx occurred during the time of connecting vertical columns, and the overflow was measured to be 2m³. The simulation results of overflow were calculated to be 1.89m³ based on the related drilling parameters of the well in the South China Sea. Good agreements between the actual data and the simulation results were observed within 5.5%.

Through the numerical simulation, the relationship between void fracture, B.H.P., and overflow can be easily obtained. And the time of gas invasion can be easily found through the calculation of B.H.P. variation with time.

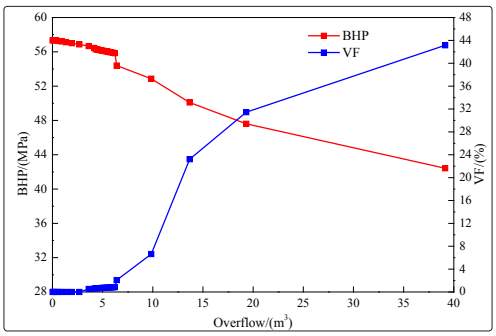

Figure 2: BHP and void fraction vs. overflow

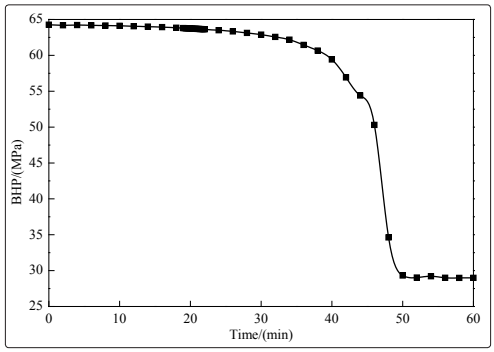

Figure 3: BHP vs. time of gas invasion

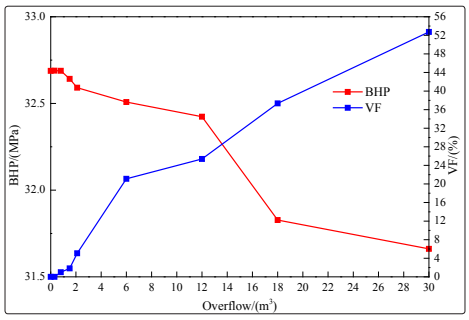

Figure 4(a): 2500 m of wellbore depth

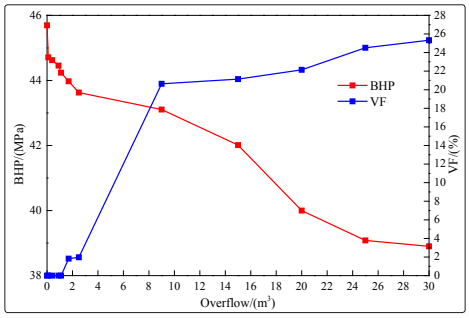

Figure 4(b): 3500 m of wellbore depth

Figure 4: BHP and void fraction vs. overflow at the different wellbore depths

According to the figure of BHP and void fraction vs. overflow and the figure of BHP vs. time of gas invasion, the degree of gas invasion can be well presented. Thus, in the actual operation in the field, no matter the gas invasion is found by means of the mud tank overflow method or by the gas rate monitoring method at the bottom section of the riser, the BHP and gas invasion time can be rapidly calculated by the software in this method after the monitoring signal response, which helps have an objective understanding of the degree of gas invasion.

The Effect of Wellbore Depth

Figure 4 shows the corresponding relationship between the BHP and void fracture and mud pool overflow under the condition that the seawater depth is 1500m and the wellbore depth is 2500m (Figure 4 (a)) and 3500m (Figure 4 (b)) when the gas invasion occurs. In Figure 4 (a), it can be easily found that when the overflow reaches $1m^3$, the void fraction at the monitoring section reaches 0.4%, and the BHP drop value is 0.07MPa. When the overflow reaches $2m^3$, the void fraction at the monitoring section reaches 3%, and the BHP drop value is 0.2MPa. At present, the accuracy of acoustic gas invasion monitoring at riser section can reach 0.1%, and the BHP decreased value is only 0.02MPa by this time, which means lower gas invasion degree at this time, and the needed mud density in well killing is low. So the risk of well control is greatly reduced. In Figure 4(b), it can be easily found that when the overflow reaches $1m^3$, the void fraction at the monitoring section reaches 0.2%, and the BHP drop value is 1.6MPa. When the overflow reaches $2m^3$, the void fraction at the monitoring section reaches 2%, and the BHP drop value is 2.2MPa. According to the present accuracy of acoustic gas invasion monitoring at riser section, the BHP decreased value is only 1.2MPa by this time, which means lower gas invasion degree at this time.

As can be seen from Figure 4, the deeper the wellbore depth, the greater the BHP drop-out value when testing the gas invasion, which means higher degree of gas invasion and more well control risk. Using the acoustic monitoring method at marine riser can fight for time for the implementation of well control measures, which can reduce the degree of gas invasion, thereby reducing the risk of well control.

The Effect of Formation Permeability

Figure 5 shows the corresponding relationship between the BHP and void fracture and mud pool overflow under the condition that the formation permeability is 100mD (Figure 5 (a)) and 300mD (Figure 5 (b)) when gas invasion occurs. The higher the formation permeability, the faster the gas rate, and the faster the increment in the mud pool. In Figure 5 (a), it can be easily found that when the overflow reaches $1m^3$, the void fraction at the monitoring section reaches 0.5%, and the BHP drop value is 4MPa. When the overflow reaches $2m^3$, the void fraction at the monitoring section reaches 8%, and the BHP drop value is 6.5MPa. According to the present accuracy of acoustic gas invasion monitoring at riser section, the BHP decreased value is only 1MPa by this time, which means lower gas invasion degree at this time and the needed mud density in well killing is low. In Figure 5(b), it can be easily found that when the overflow reaches $1m^3$, the void fraction at the monitoring section reaches 0.02%, and the BHP drop value is 0.2MPa. When the overflow reaches $2m^3$, the void fraction at the monitoring section reaches 0.03%, and the BHP drop value is 0.4MPa. According to the present accuracy of acoustic gas invasion monitoring at riser section, the BHP decreased value is 0.9MPa by this time, which means higher gas invasion degree at this time. So the needed mud density in well killing is higher and the risk of well control increases.

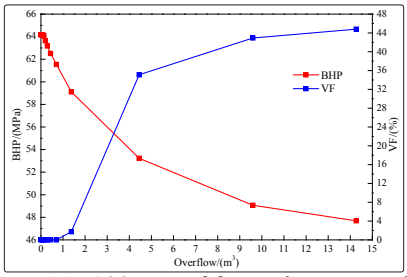

Figure 5(a): 100 mD of formation permeability

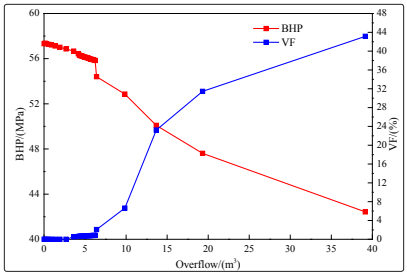

Figure 5(b): 300 mD of formation permeability

Figure 5: BHP and void fraction vs. overflow at different formation permeability

As can be seen from Figure 5, the greater the permeability, the greater the BHP drop-out value when testing the gas invasion, which means higher degree of gas invasion and more well control risk. When the formation permeability is low, the use of acoustic monitoring method at marine riser can fight for time for the implementation of well control measures, which can reduce the degree of gas invasion, thereby reducing the risk of the well control. When the formation permeability is high, then the method of acoustic monitoring has no advantage.

The Effect of Formation Equivalent Density

Figure 6 shows the corresponding relationship under the condition that the formation equivalent density is 1330 kg/m^3 (Figure 6(a)) and 1350 kg/m^3 (Figure 6 (b)) when the gas invasion occurs. In Figure 6(a), it can be easily found that when the overflow reaches 1m^3, the void fraction at the monitoring section reaches 0.5%, and the BHP drop value is 4MPa. When the overflow reaches 2m^3, the void fraction at the monitoring section reaches 8%, and the BHP drop value is 6.5MPa. According to the present accuracy of acoustic gas invasion monitoring at riser section, the BHP decreased value is only 1MPa by this time, which means lower gas invasion degree at this time, and the needed mud density in well killing is low. In Figure 6(b), it can be easily found that when the overflow reaches 1m3, the void fraction at the monitoring section reaches 0.01%, and the BHP drop value is 2MPa. When the overflow reaches 2m3, the void fraction at the monitoring section reaches 0.02%, and the BHP drop value is 3MPa.

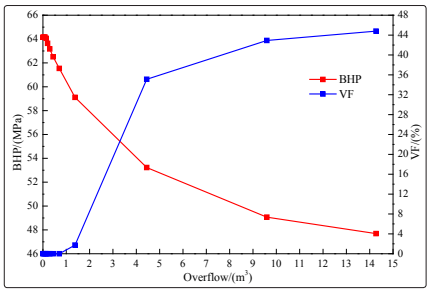

Figure 6(a):1330 kg/m^3 of equivalent density

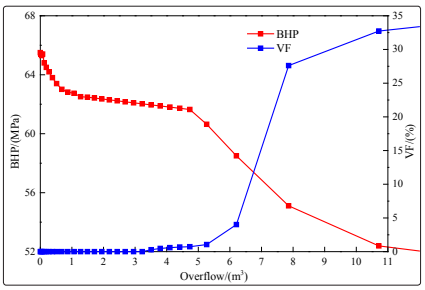

Figure 6(b): 1350 kg/m^3 of equivalent density

Figure 6: BHP and void fraction vs. overflow at different formation equivalent densities

As can be seen from Figure 6, the effect of formation equivalent density is similar to the formation permeability. When the formation equivalent density is low, the use of acoustic monitoring method at marine riser can fight for time for the implementation of the well control measures, which can reduce the degree of gas invasion, thereby reducing the risk of well control. When the formation equivalent density is high, then the method of acoustic monitoring has no advantage.

Conclusions

In this paper, through the establishment of the gas-liquid two-phase flow model, a real-time quantitative relationship between the BHP and void fraction at bottom section and mud tank overflow is established. Then, the change rule between the BHP and void fraction and the mud tank overflow can be obtained under conditions of different well depth, permeability, and formation pressure. The deeper the wellbore depth, the greater the BHP drop-out value. When the formation permeability is low, the use of acoustic monitoring method at marine riser can fight for time for the implementation of well control measures. When the formation permeability is high, then the method of acoustic monitoring has no advantage. The greater the equivalent density, the greater the BHP drop-out value when testing the gas invasion. The effect of formation equivalent density is the same as formation permeability.

Acknowledgments

The authors gratefully thank the member companies of the down hole System Information and Control Center at China University of Petroleum (East China). The National Natural Science Fund of China (Grants 51574275), the Fundamental Research Funds for the Central Universities (Grants 17CX06016) and the National Natural Science Funds Youth Fund(Grants 51704320) supported this work.

References

1. Yang Jinhua (2014) The status and prospect of global deepwater drilling. Oil Forum 33: 46-50.
2. Sun BJ, Cao SH J, Li H, SHANG ZK (2011) Status and Development Trend of Deepwater Drilling Technology and Equipment. Petroleum Drilling Technology 39: 8-15.
3. Geng YN (2016) Study on real-time ultra-sonic kick detection technique along riser during deep water drilling operations. China Offshore Oil and Gas 28: 86-92.
4. Zhang K (2013) Developing oil and gas from deep waters with the self-manufactured equipment. Acta PetroleiSinica 34: 802-808.
5. Fu Jianhong, Feng Jian, Chen Ping, Wei Hongshu, Liu Zhengli (2015) Simulation on wellbore pressure during dynamics kill

drilling in deep water. Acta PetroleiSinica 36: 232-237.
6. Hauge S, Qien K (2012) Deepwater Horizon: Lessons learned for the Norwegian petroleum industry with focus on technical aspects. Chemical Engineering Transactions 26: 621-626.
7. Cheng R, Wang H (2013) Drilling risk management in offshore china: insights and lessons learned from the deepwater horizon incident, IPTC 16726.
8. Skogdalen JE, Utne IB, Vinnem JE (2012) Quantitative risk analysis of oil and gas drilling, using deepwater horizon as case study. Reliability Engineering & System Safety 100: 58-66.
9. Hargreaves D, Jardine S, Jeffryes B (2001) Early kick detection for deep-water drilling: new probabilistic methods applied in the field. SPE 71369.
10. Toralde JSS, Wuest CH (2014) Riser Gas Risk Mitigation with Advanced Flow Detection and Managed Pressure Drilling Technologies in Deepwater Operations. Higher Education Reforms in Romania. Springer International Publishing.
11. Jonggeun C, Schubert JJ, Juvkam-Wold HC (2007) Analyses and procedures for kick detection in subsea mudlift drilling. Spe Drilling & Completion 22: 296-303.
12. Ghajar AJ, Bhagwat SM (2014) Flow Patterns, Void Fraction and Pressure Drop in Gas-Liquid Two Phase Flow at Different Pipe Orientations. Frontiers and Progress in Multiphase Flow I.
13. Avelar CS, Ribeiro PR, Sepehrnoori K (2009) Deep water gas kick simulation. J Journal of Petroleum Science & Engineering 67: 13-22.
14. Wang Z (2014) Deep water gas kick simulation with consideration of the gas hydrates phase transition. J Journal of Hydrodynamics B 26: 94-103.
15. Nickens HV (1987) A dynamic computer model of a kicking well. Spe Drilling Engineering 2: 159-173.
16. Hauge E, Aamo OM, Godhavn JM, Nygaard G (2013) A novel model-based scheme for kick and loss mitigation during drilling. Journal of Process Control 23: 463-472.
17. Apak EC, Ozbayoglu EM (2009) Heat distribution within the wellbore while drilling. Petroleum Science & Technology 27: 678-686.
18. Imamura Y, Yamada H, Ikushima T, Shakutsui H (2006) Pressure drop of gas-liquid two-phase flow in a large diameter vertical pipe. Research Memoirs of the Kobe Technical College 44: 19-24.
19. Orkiszewski J (2013) Predicting two-phase pressure drops in vertical pipe. Journal of Petroleum Technology 19: 829-838.
20. Gao YH (2007) Study on Multi-phase Flow in Wellbore and Well Control in Deep Water Drilling, China. Ph.D. thesis China University of Petroleum (East China), Qingdao, China.